NASA TECHNICAL NOTE

NASA TN D-5508
c. 1

NASA TN D-5508

EXPERIMENTAL INVESTIGATION OF FLUTTER AT MACH 3 OF ROTATIONALLY RESTRAINED PANELS AND COMPARISON WITH THEORY

by Charles P. Shore

Langley Research Center
Langley Station, Hampton, Va.

NATIONAL AERONAUTICS AND SPACE ADMINISTRATION • WASHINGTON, D. C. • OCTOBER 1969

1. Report No. NASA TN D-5508	2. Government Accession No.	3. Recipient's Catalog No.
4. Title and Subtitle EXPERIMENTAL INVESTIGATION OF FLUTTER AT MACH 3 OF ROTATIONALLY RESTRAINED PANELS AND COMPARISON WITH THEORY		5. Report Date October 1969
		6. Performing Organization Code
7. Author(s) Charles P. Shore		8. Performing Organization Report No. L-6322
		10. Work Unit No. 126-14-14-06-23
9. Performing Organization Name and Address NASA Langley Research Center Hampton, Va. 23365		11. Contract or Grant No.
		13. Type of Report and Period Covered Technical Note
12. Sponsoring Agency Name and Address National Aeronautics and Space Administration Washington, D.C. 20546		
		14. Sponsoring Agency Code

15. Supplementary Notes A part of the information presented herein was included in a thesis entitled "Flutter of Stressed Panels Including Effects of Edge Rotational Restraint and Damping" submitted in partial fulfillment of the requirements for the degree of Master of Science in Engineering Mechanics, Virginia Polytechnic Institute, Blacksburg, Virginia, March 1967.

16. Abstract

An experimental investigation was conducted at a Mach number of 3 in the Langley 9- by 6-foot thermal structures tunnel to study the effects of damping and edge rotational restraint on the flutter characteristics of thermally stressed, flat, isotropic panels with length-width ratios of 3.3 and 3.7. Measured panel natural vibration frequencies were compared with calculated frequencies in order to estimate the panel edge rotational restraints. Comparisons of experimental and theoretical flutter results show that small-deflection theory can adequately predict the flutter of stressed panels up to the point of buckling if edge rotational restraint is accounted for and aerodynamic damping and frequency-independent hysteretic structural damping are included. Furthermore, the region, where the theoretical transition-point value of the flutter parameter is very sensitive to variations in panel length-width ratio and edge rotational restraint when structural damping is zero, becomes insensitive to these variations when the appropriate value of structural damping is used.

17. Key Words Suggested by Author(s) Buckling Vibration Flutter Rectangular panels	18. Distribution Statement Unclassified – Unlimited		
19. Security Classif. (of this report) Unclassified	20. Security Classif. (of this page) Unclassified	21. No. of Pages 32	22. Price* $3.00

*For sale by the Clearinghouse for Federal Scientific and Technical Information
Springfield, Virginia 22151

EXPERIMENTAL INVESTIGATION OF FLUTTER AT MACH 3
OF ROTATIONALLY RESTRAINED PANELS AND
COMPARISON WITH THEORY*

By Charles P. Shore
Langley Research Center

SUMMARY

An experimental investigation was conducted at a Mach number of 3 in the Langley 9- by 6-foot thermal structures tunnel to study the effects of damping and edge rotational restraint on the flutter characteristics of thermally stressed, flat, isotropic panels with length-width ratios of 3.3 and 3.7. Measured panel natural vibration frequencies were compared with calculated frequencies in order to estimate the panel edge rotational restraints. Comparisons of experimental and theoretical flutter results show that small-deflection theory can adequately predict the flutter of stressed panels up to the point of buckling if edge rotational restraint is accounted for and aerodynamic damping and frequency-independent hysteretic structural damping are included. Furthermore, the region, where the theoretical transition-point value of the flutter parameter is very sensitive to variations in panel length-width ratio and edge rotational restraint when structural damping is zero, becomes insensitive to these variations when the appropriate value of structural damping is used.

INTRODUCTION

Better understanding of the flutter of stressed panels has resulted from the consideration of edge rotational restraint and damping in panel flutter theory and experiment. (See, for example, refs. 1 to 3.) In reference 2, accounting for the effects of edge rotational restraint was found to improve agreement between theoretical and experimental results for stressed panels. In reference 3, it was shown that the use of structural damping represented in a manner consistent with the representation for a Kelvin-Voigt

---

*A part of the information presented herein was included in a thesis entitled "Flutter of Stressed Panels Including Effects of Edge Rotational Restraint and Damping" submitted in partial fulfillment of the requirements for the degree of Master of Science in Engineering Mechanics, Virginia Polytechnic Institute, Blacksburg, Virginia, March 1967.

viscoelastic body removes the physically untenable results that plagued earlier flutter analyses and further improved the agreement between theoretical and experimental results. However, additional data are needed for further substantiation of the theory of reference 3.

In the present experimental investigation, panels with length-width ratios of 3.3 and 3.7 were tested at a Mach number of 3 in the Langley 9- by 6-foot thermal structures tunnel to obtain flutter boundaries for panels with different degrees of edge rotational restraint. Measured panel natural vibration frequencies were compared with calculated frequencies in order to estimate the edge rotational restraint for each panel. The panels were grouped according to the degree of edge rotational restraint. For a given group of panels, the variation of edge rotational restraint was considered sufficiently small to allow the use of an average value which would not preclude a valid comparison with theory. Values of structural damping were estimated from the results presented in reference 4 for material damping and in references 5 and 6 for boundary-support damping. The experimental flutter boundaries are shown to be in good agreement with theoretical flutter boundaries calculated from the small-deflection theory of reference 3. In addition, the experimental results for panels stressed to buckling in references 2 and 7 to 9 and the present investigation are shown to substantiate the theoretical trends of variations of edge rotational restraint and length-width ratio indicated by the theory of reference 3.

SYMBOLS

The units used for the physical quantities in this paper are given both in the U.S. Customary Units and in the International System of Units (SI). Factors relating the two systems are given in reference 10, and those used in the present investigation are presented in the appendix.

a   panel length

B   panel frame width

b   panel width

C   empirical proportionality constant

c   free-stream speed of sound

D   bending stiffness of isotropic panel, $\dfrac{Eh^3}{12(1 - \mu^2)}$

E   Young's modulus

f   flutter frequency

f_n natural frequency for nth longitudinal mode,   n = 1, 2, 3, 4

f_o first natural frequency of simply supported semi-infinite plate, $\dfrac{\pi}{2a^2}\sqrt{\dfrac{D}{\gamma h}}$

g   frequency-independent hysteretic structural damping coefficient

g_a aerodynamic damping coefficient, $\dfrac{\rho c}{2\pi\gamma f_o}$

h   panel thickness

k_x nondimensional stress coefficient in x-direction, $\dfrac{N_x a^2}{\pi^2 D}$

M   Mach number

N_x inplane loading in x-direction, positive in compression

N_y inplane loading in y-direction, positive in compression

p_t free-stream stagnation pressure

Δp static differential pressure acting on panel skin

q   free-stream dynamic pressure

q_x rotational restraint coefficient on boundaries   x = 0   and   x = a, $\dfrac{a\theta_x}{D}$

q_y rotational restraint coefficient on boundaries   y = 0   and   y = b, $\dfrac{b\theta_y}{D}$

T   panel skin temperature

T_t free-stream stagnation temperature

ΔT average increase of panel skin temperature

t   time

x,y	Cartesian coordinates of panel (see fig. 1)
α	coefficient of thermal expansion of panel skin
β	compressibility factor, $\sqrt{M^2 - 1}$
γ	panel mass per unit area
θ_x	rotational spring constant along boundaries $x = 0$ and $x = a$
θ_y	rotational spring constant along boundaries $y = 0$ and $y = b$
μ	Poisson's ratio for isotropic panel
ρ	free-stream air density
ψ	modified temperature parameter (see eq. (1))

Subscripts:

av	average
T	transition point

EXPERIMENTAL INVESTIGATION

Panels

The 2024-T3 aluminum-alloy test panels of various thicknesses were riveted to thick frames of the same material. The test panels were insulated from the frames by a 0.031-inch (0.08-cm) strip of fiber-glass cloth. In order to reduce initial stresses due to mounting, the test panels were riveted after the frames were bolted to the mounting fixture used in the tests. Panel construction details and the mounting arrangement are shown in figures 1 to 4. The panels were 26 inches (66 cm) long and 7.88 or 7.03 inches (20.1 or 17.9 cm) wide which corresponded to length-width ratios of 3.3 and 3.7. A total of nine panels with a length-width ratio of 3.3 and thicknesses ranging from 0.052 to 0.102 inch (0.132 to 0.259 cm) were tested. Two panels with a length-width ratio of 3.7 and thicknesses of 0.054 and 0.064 inch (0.137 and 0.162 cm) were tested.

Test Apparatus

Tunnel.- All tests were conducted in the Langley 9- by 6-foot thermal structures tunnel, a Mach 3 intermittent blowdown facility exhausting to the atmosphere. A heat exchanger is preheated to provide stagnation temperatures up to 660° F (620° K). The stagnation pressure can be varied from 60 to 200 psia (410 to 1380 kN/m^2). Additional details on the tunnel are presented in reference 11.

Panel holder and mounting arrangement.- The panel holder has a beveled half-wedge leading edge with a cavity on the nonbeveled side 29 inches (74 cm) wide, 30 inches (76 cm) high, and 5 inches (13 cm) deep for accommodating test specimens. (See figs. 2 and 3.) Instrumentation in the cavity and instrumentation chamber reduces the effective depth of the cavity to approximately 3.5 inches (9 cm). Pheumatically operated sliding doors protect test specimens from aerodynamic buffeting and heating during tunnel start and shutdown. Aerodynamic fences prevent shock waves emanating from the doors from interfering with the airflow over the test specimen. The results of pressure surveys indicate that the flow conditions over the exposed surface of a flat panel are essentially free-stream conditions (ref. 11). A manually operated vent door on the side opposite the cavity is used to control the pressure inside the cavity behind the test specimen. (See fig. 3.) All other openings to the cavity are sealed.

All test panels were mounted flush with the flat surface of the panel holder. The test panels and associated filler plates were attached by screws to the mounting fixture which had been bolted to the panel holder. (See figs. 3 and 4.)

Instrumentation

Iron-constantan thermocouples, spotwelded to the back of the panel skins at 19 locations (see fig. 5), were used to measure panel temperatures. Variable-reluctance-type deflectometers were used to detect motion of the panel skin and to measure panel frequencies. The deflectometers were located in the cavity approximately 0.25 inch (0.6 cm) behind the panel at the three positions indicated in figure 5. In addition, high-speed 16-mm motion pictures provided supplementary data on the behavior of the panels. Grid lines were painted on the panels to facilitate visual analysis of the motion pictures.

Quick-response strain-gage-type pressure transducers were used to measure static pressure at various locations on the panel holder and in the cavity behind the panel. Stagnation pressures in the test section were obtained from static-pressure measurements in the tunnel settling chamber. Stagnation temperatures were measured by total-temperature probes located in the test section. For each test, data from the thermocouples and pressure transducers were recorded on magnetic tape every twentieth of a second. Deflectometer readings were recorded on a high-speed oscillograph.

Test Procedure

The panels were vibrated at sea-level conditions in the panel holder prior to each test by using an air-jet shaker which is described in reference 12. Several panels attached to the mounting fixture were also vibrated prior to installation in the panel holder, the cavity behind the panels being effectively infinite. Comparison of the results showed that the effect of change in cavity depth on the panel natural vibration frequencies was negligible.

Prior to the wind-tunnel flutter tests, a flat calibration panel was installed in the panel holder and pressure surveys similar to those in reference 11 were conducted to determine the flow conditions over the test cavity. The results indicated that the flow conditions were essentially free-stream conditions. A pressure-orifice location along the leading edge of the test cavity which gave a reading that most nearly matched the average pressure reading over the calibration panel and a pressure-orifice location in the test cavity which gave a reading that most nearly matched the average pressure reading of the internal cavity were used to determine the value of Δp across the test panels.

The wind-tunnel flutter tests were conducted at a Mach number of 3, at stagnation pressures from 58 to 199 psia (400 to 1370 kN/m^2), and at stagnation temperatures from 300° F to 504° F (420° K to 540° K). The protective doors on the panel holder were opened after the desired test conditions were established and were closed 3 seconds prior to tunnel shutdown. The duration of the tests varied from 10 to 40 seconds. The stagnation temperature was nearly constant during each test. The differential pressure Δp was maintained as near zero as possible by manual control of the cavity vent-door position. The stagnation pressure was held constant during the first few seconds of each test. It was then varied in order to obtain as many flutter points as practical. Flutter was readily determined by monitoring the deflectometer traces on the high-speed oscillograph during the tests. The usual procedure for varying the stagnation pressure was as follows:

(1) If flutter had not occurred after a predetermined period of time, the test was either ended or the stagnation pressure was increased in an attempt to initiate flutter.

(2) If flutter had started and stopped, the stagnation pressure was increased in an attempt to restart flutter.

(3) If the panel was still fluttering after a predetermined period of time, the stagnation pressure was decreased in an attempt to stop flutter.

RESULTS AND DISCUSSION

Edge Rotational Restraint Coefficients

The panel natural vibration frequencies measured in the panel holder prior to each test are presented in table I. The mode shapes associated with the four frequencies f_n recorded during the vibration tests consisted of one half-wave in the cross-stream direction and n half-waves in the streamwise direction. Values for the edge rotational restraint coefficients were determined by comparing the measured panel natural vibration frequencies with calculated frequencies. The analysis of reference 3 was used to calculate the variation of the first two natural frequencies with q_x for both length-width ratios. Because the edge attachments were the same on all edges, equal rotational restraints were assumed; that is, $\theta_x = \theta_y$. Thus, the nondimensional edge rotational restraint coefficients $q_x = \dfrac{a\theta_x}{D}$ and $q_y = \dfrac{b\theta_y}{D}$ are related through the length-width ratio by $q_y = \dfrac{b}{a} q_x$.

Figure 6 shows the variation of the first two natural frequencies with edge rotational restraint as determined from reference 3 for the panels with a length-width ratio of 3.3; a value of $q_x = 0$ corresponds to simply supported edges and a value of $q_x = \infty$ corresponds to clamped edges. Values of q_x were determined from figure 6 for each of the first two measured frequencies of the test panels. Since panel flutter is usually more dependent on the two lowest panel natural vibration frequencies, the average value of q_x obtained for the first two modes was used as the value of the edge rotational restraint coefficient for a given test. A similar procedure was followed for the panels with a length-width ratio of 3.7. The values of q_x for the first two measured frequencies and the resulting average values are given in table I.

Flutter Results

The results of the flutter tests are presented in tables II and III in terms of the panel and wind-tunnel conditions for flutter. The tabulated data include the free-stream stagnation temperature T_t, free-stream stagnation pressure p_t, free-stream dynamic pressure q, static differential pressure Δp, panel-skin-temperature increase ΔT, and flutter frequency f.

Panel temperatures.- The panel skin and supporting structure were at the same temperature before the panel was exposed to the airstream. After exposure, the skin temperature increased as shown by the typical panel temperature history in figure 7. The upper curve consists of the average readings of thermocouples located on or near the panel center line. The two lower curves consist of the average readings of thermocouples near and adjacent to the panel edges. The differences indicate temperature gradients near

the panel edges. These gradients are attributed to heat conduction to the supporting structure but were neglected in the analysis of the test data. The panel-temperature increase ΔT was taken as the difference between the average reading of the center-line thermocouples at the time of flutter and the average reading of the center-line thermocouples at the time the protective doors were opened.

Flutter parameters.- The flutter-start points (denoted as panel flat in table II) for the panels with a length-width ratio of 3.3 are plotted in figure 8. The flutter-start points are presented in terms of a dimensionless dynamic-pressure flutter parameter and a dimensionless temperature parameter. The flutter parameter $\left(\dfrac{q}{\beta E}\right)^{1/3} \dfrac{a}{h}$ relates the dynamic pressure required for flutter to the panel stiffness, length, and thickness and includes the effect of Mach number through the compressibility factor β. Only the dynamic pressure q and thickness h were varied in these tests. Changes in material properties with temperature were assumed to be negligible because of the relatively low panel temperatures and short duration of the tests. The temperature parameter $\alpha \, \Delta T \left(\dfrac{a}{h}\right)^2$ gives an indication of the midplane loading in the stream direction. The large amount of scatter exhibited by the data in figure 8 prevents the establishment of a distinct flutter boundary. This scatter is attributed to two factors: (1) the effects of edge rotational restraint and (2) the membrane loading introduced by the differential pressure acting over the panel.

The effects of edge rotational restraint were accounted for by grouping the data shown in figure 8 according to the values of q_x. For the panels with a length-width ratio of 3.3, three reasonably distinct groups resulted. These groups are $q_{x,av} = 40, 80,$ and ∞. The flutter data for these panels are given in table II and are identified by the average value of q_x for each group, denoted by $q_{x,av}$. Individual values of q_x did not vary widely for the $q_{x,av} = 40$ and $q_{x,av} = 80$ tests. In the third group, table II(c), values of q_x ranged from 108 to ∞. However, reference 3 shows that these panels are theoretically insensitive to q_x beyond $q_x = 100$ and these panels were therefore assumed to be effectively clamped. The panels with a length-width ratio of 3.7 were found to be effectively clamped $\left(q_{x,av} = \infty\right)$; the flutter data for these panels are given in table III.

The membrane load due to differential pressure was approximated by the following expression (see ref. 7):

$$\frac{12(1 + \mu)}{\pi^2} \, C\left[\frac{|\Delta p|}{E}\left(\frac{a}{h}\right)^4\right]^{2/3}$$

Combining the preceding expression with the temperature parameter gives the following expression which is a measure of the total midplane loading:

8

$$\psi = \frac{12(1 + \mu)}{\pi^2} \left\{ \alpha \, \Delta T \left(\frac{a}{h}\right)^2 \pm C \left[\frac{|\Delta p|}{E} \left(\frac{a}{h}\right)^4 \right]^{2/3} \right\} \qquad (1)$$

This expression has been called the modified temperature parameter. In the parameter, the minus sign applies when a panel is unbuckled because a differential pressure causes tension. The plus sign applies when a panel is buckled, and ψ is then a measure of buckle depth. A detailed discussion of the parameter ψ is given in reference 7. The factor C is a proportionality constant that can be determined from the experimental data by the procedure developed in reference 7; values of C determined for each group of test data are given in tables II and III.

The data in figure 8 are replotted in figure 9 in terms of the parameter ψ which includes the effects of Δp. These data are also grouped according to the values of $q_{x,av}$. Use of the parameter ψ removes most of the extreme scatter in the data and permits assessment of the effect of an increase in the edge rotational restraint. The overall effect of an increase in $q_{x,av}$ is a shift of the boundary to the right in terms of ψ which results in an increase in the panel buckling load. Removal of the extreme scatter by accounting for the membrane loading induced by Δp and by grouping the data according to the average value of the edge rotational restraint coefficient permits establishment of three reasonably distinct flutter boundaries for the panels with a length-width ratio of 3.3.

Flutter boundaries.- The flutter boundaries, in terms of the flutter parameter as a function of the modified temperature parameter, are shown in figures 10 and 11 for the panels with length-width ratios of 3.3 and 3.7, respectively. In figures 10 and 11, flutter-start points (panel flat) are shown by the open symbols and flutter-stop points (panel buckled) by solid symbols. In addition, a flutter-start point (panel buckled) is shown by an open symbol with a flag in figure 11. The curves faired through the data points are boundaries above which the panels fluttered. The panel-flat boundary and the panel-buckled boundary intersect at a transition point where the slope changes from negative to positive. The positive slope of the boundary is attributed to an increase in stiffness as the buckle depth increases. The general trend of each boundary is similar to previous experimental results. (See, for example, refs. 2, 7, and 8.)

The flutter motion observed from high-speed motion pictures appeared to be of the traveling-wave type. The flutter mode shape appeared to have two half-waves in the streamwise direction and one half-wave in the cross-stream direction. Buckled mode shapes were similar to the flutter mode shapes. This similarity has been noted previously in references 9 and 11.

COMPARISON OF THEORY AND EXPERIMENT

The panel-flat flutter boundaries in figures 10 and 11 are replotted in figures 12 and 13 as a function of the ratio ψ/ψ_T where the subscript T indicates the transition-point value. Theoretical boundaries, calculated from the small-deflection theory of reference 3, are shown for comparison in terms of $k_x/k_{x,T}$. The ratios ψ/ψ_T and $k_x/k_{x,T}$ are equivalent. The theory of reference 3 accounts for arbitrary edge rotational restraints. The lower theoretical curves in these figures were calculated for zero damping. The upper theoretical curves were obtained for values of the aerodynamic damping coefficient g_a calculated from the test conditions and for an estimated value of the frequency-independent hysteretic structural damping coefficient g of 0.01. This estimate is based on the results of references 5 and 6, which revealed that damping mechanisms at panel boundaries can increase the value of structural damping up to five times the value of material damping. The value of material damping for an alloy similar to that used in the present investigation is 0.003. (See ref. 4.)

Agreement between the experimental boundaries and those predicted by the theory for zero damping is reasonable for moderate inplane loadings but becomes poor in the region of the transition point where the theory predicts physically unreasonable results. However, when structural damping and aerodynamic damping are included in the theoretical calculations, the agreement is good along the entire boundary.

The transition-point values of the flutter parameter for the panels with a length-width ratio of 3.3 are compared with theoretical transition-point values from reference 3 in figure 14 to show the effects of edge rotational restraint. The lower curve was calculated for zero damping and the upper curve was calculated for a structural damping coefficient g of 0.01. The circular symbols are the experimental transition points from figure 10. The experimental data substantiate the trend predicted by the theory for $g = 0.01$.

The effects of a/b on the transition-point values of the flutter parameter, expressed in terms of the panel width b, are shown in figure 15 for fully clamped panels with $N_y/N_x = 1$. The theoretical curves were calculated from the analysis of reference 3 for $g = 0$ and 0.01. The experimental transition-point values of the flutter parameter for panels considered effectively clamped were obtained from two flutter boundaries of the present investigation and from references 2 and 7 to 9. The theoretical curves indicate a marked decrease in the transition-point value of the flutter parameter as a/b increases from 1 to about 2.5; however, the curve for $g = 0.01$ tends to become horizontal in this region and indicates very little further decrease as a/b increases beyond $a/b = 2.5$. Thus, in this region the flutter parameter becomes independent of the panel

length a. The experimental data points follow the trend predicted by the curve for g = 0.01 which gives a conservative estimate of the flutter parameter.

The theoretical and experimental results shown in figures 14 and 15 indicate that the region, where the theoretical transition-point value of the flutter parameter is very sensitive to variations in length-width ratio and edge rotational restraint when g = 0, becomes insensitive to these variations when the appropriate value of g is used. The ability to predict experimental results with reasonable accuracy at the transition point coupled with the insensitivity of the transition point to variations in length-width ratio and edge rotational restraint suggests the possibility of placing panel flutter design on an analytical basis. And, in fact, flutter design charts for isotropic panels that are on the verge of buckling are developed in reference 13.

CONCLUSIONS

An experimental investigation was conducted at a Mach number of 3 in the Langley 9- by 6-foot thermal structures tunnel to study the effects of edge rotational restraint and damping on the flutter characteristics of thermally stressed, flat, isotropic panels with length-width ratios of 3.3 and 3.7. The experimental results and results from other investigations were compared with theoretical results from a small-deflection theory which accounts for arbitrary edge rotational restraints and includes frequency-independent hysteretic structural damping as well as aerodynamic damping. The experimental results and comparisons with the theory revealed the following:

1. Establishment of distinct experimental flutter boundaries with little scatter is dependent on proper account of panel edge rotational restraint and midplane loading including the influence of differential pressure.

2. Good agreement between theoretical and experimental panel-flat flutter boundaries can be obtained when edge rotational restraint is accounted for and when appropriate values of aerodynamic damping and structural damping are included in the theoretical calculations.

3. The region, where the theoretical transition-point value of the flutter parameter is very sensitive to variations in panel length-width ratio and edge rotational restraint when the structural damping is zero, becomes insensitive to these variations when the appropriate value of structural damping is used.

Langley Research Center,
    National Aeronautics and Space Administration,
        Langley Station, Hampton, Va., August 4, 1969.

APPENDIX

CONVERSION OF U.S. CUSTOMARY UNITS TO SI UNITS

Factors required for converting the units used herein to the International System of Units (SI) are given in the following table:

Physical quantity	U.S. Customary Units	Conversion factor (*)	SI Unit (**)
Length	in.	0.0254	meters (m)
Pressure	psi = lbf/in^2	6.895×10^3	newtons/meter^2 (N/m^2)
Temperature . . .	°F	$\frac{5}{9}$(F + 459.67)	degrees Kelvin (°K)

*Multiply value given in U.S. Customary Unit by conversion factor to obtain equivalent value in SI Unit.

**Prefixes to indicate multiples of SI units are as follows:

Prefix	Multiple
giga (G)	10^9
kilo (k)	10^3
centi (c)	10^{-2}
milli (m)	10^{-3}

REFERENCES

1. Erickson, Larry L.: Supersonic Flutter of Flat Rectangular Orthotropic Panels Elastically Restrained Against Edge Rotation. NASA TN D-3500, 1966.

2. Shideler, John L.; Dixon, Sidney C.; and Shore, Charles P.: Flutter at Mach 3 of Thermally Stressed Panels and Comparison With Theory for Panels With Edge Rotational Restraint. NASA TN D-3498, 1966.

3. Shore, Charles P.: Effects of Structural Damping on Flutter of Stressed Panels. NASA TN D-4990, 1969.

4. Granick, Neal; and Stern, Jesse E.: Material Damping of Aluminum by a Resonant-Dwell Technique. NASA TN D-2893, 1965.

5. Mentel, T. J.; and Schultz, R. L.: Viscoelastic Support Damping of Built-In Circular Plates. ASD-TDR-63-648, U.S. Air Force, Oct. 1963.

6. Ungar, Eric E.: Energy Dissipation at Structural Joints; Mechanisms and Magnitudes. FDL-TDR-64-98, U.S. Air Force, Aug. 1964.

7. Dixon, Sidney C.: Experimental Investigation at Mach Number 3.0 of Effects of Thermal Stress and Buckling on Flutter Characteristics of Flat Single-Bay Panels of Length-Width Ratio 0.96. NASA TN D-1485, 1962.

8. Dixon, Sidney C.; and Shore, Charles P.: Effects of Differential Pressure, Thermal Stress, and Buckling on Flutter of Flat Panels With Length-Width Ratio of 2. NASA TN D-2047, 1963.

9. Dixon, Sidney C.: Application of Transtability Concept to Flutter of Finite Panels and Experimental Results. NASA TN D-1948, 1963.

10. Comm. on Metric Pract.: ASTM Metric Practice Guide. NBS Handbook 102, U.S. Dep. Com., Mar. 10, 1967.

11. Dixon, Sidney C.; Griffith, George E.; and Bohon, Herman L.: Experimental Investigation at Mach Number 3.0 of the Effects of Thermal Stress and Buckling on the Flutter of Four-Bay Aluminum Alloy Panels With Length-Width Ratios of 10. NASA TN D-921, 1961.

12. Herr, Robert W.; and Carden, Huey D.: Support Systems and Excitation Techniques for Dynamic Models of Space Vehicle Structures. Proceedings of Symposium on Aeroelastic & Dynamic Modeling Technology, RTD-TDR-63-4197, Pt. I, U.S. Air Force, Mar. 1964, pp. 249-277.

13. Shore, Charles P.: Flutter Design Charts for Stressed Isotropic Panels. Volume of Technical Papers on Structural Dynamics, Amer. Inst. Aeronaut. Astronaut., 1969, pp. 296-301.

TABLE I.- NATURAL FREQUENCIES MEASURED PRIOR TO EACH TEST FOR TEST PANELS MOUNTED IN PANEL HOLDER

(a) a/b = 3.3

Panel	Test	h in.	h mm	f_1, Hz	f_2, Hz	f_3, Hz	f_4, Hz	q_x for f_1	q_x for f_2	q_x for test
1	1	0.052	1.32	160	183	215	267	64	86	75
2	2	0.053	1.35	203	212	249	299	∞	∞	∞
	3			195	212	262	323	∞	∞	∞
	4			184	194	234	291	315	115	215
3	5	0.054	1.37	183	201	232	282	200	200	200
	6			172	188	227	282	89	80	85
	7			167	188	221	277	68	80	74
	*8			---	---	---	---	---	---	---
4	9	0.055	1.4	177	191	218	274	98	77	87
	10			141	184	191	225	15	52	34
	11			164	179	214	271	47	43	45
5	12	0.063	1.6	205	234	286	348	108	188	148
	13			203	227	273	332	100	116	108
	14			198	215	263	328	78	65	71
6	15	0.065	1.65	218	236	287	348	164	130	147
	16			215	236	286	353	133	133	133
7	17	0.076	1.93	242	286	325	402	95	200	147
	18			263	290	331	416	333	333	333
8	19	0.080	2,03	236	275	343	398	43	55	49
	20			220	263	301	377	26	44	35
	21			224	270	309	384	28	52	40
	22			216	267	310	385	27	49	38
	*23			---	---	---	---	---	---	---
9	24	0.102	2.59	326	352	416	508	91	74	83
	25			333	362	426	517	116	100	108
	26			323	348	412	505	84	66	75
	27			326	358	420	515	93	89	91
	28			323	350	411	504	85	69	77
	29			330	346	410	505	112	62	87

*Frequency not obtained prior to test.

TABLE I.- NATURAL FREQUENCIES MEASURED PRIOR TO EACH TEST
FOR TEST PANELS MOUNTED IN PANEL HOLDER — Concluded

(b) a/b = 3.7

| Panel | Test | h | | f_1, Hz | f_2, Hz | f_3, Hz | f_4, Hz | q_x for — | | q_x for test |
		in.	mm					f_1	f_2	
10	1	0.054	1.37	255	280	319	365	400	∞	∞
	2			235	260	284	343	364	∞	∞
	*3			---	---	---	---	----	----	----
	4			235	280	301	354	364	∞	∞
11	5	0.064	1.62	287	308	350	417	2000	4000	3000
	6			276	315	351	415	308	∞	∞
	7			263	294	325	386	133	250	191
	8			268	306	341	402	167	1142	654
	9			261	297	331	393	121	307	214

*Frequency not obtained prior to test.

TABLE II.- PANEL FLUTTER TEST DATA FOR $a/b = 3.3$

$$\left[E = 10.5 \times 10^6 \text{ psi} \quad (72.4 \text{ GN/m}^2); \quad \alpha = 12.6 \times 10^{-6} \text{ }^\circ\text{F}^{-1} \quad (22.7 \times 10^{-6} \text{ }^\circ\text{K}^{-1})\right]$$

(a) $q_{x,av} = 40$; $q_{y,av} = 12$; $C = 0.86$

Test	h (in.)	h (mm)	T_t (°F)	T_t (°K)	p_t (psia)	p_t (kN/m²)	q (psi)	q (kN/m²)	Δp (psi)	Δp (kN/m²)	ΔT (°F)	ΔT (°K)	f, Hz	g_a	$\alpha \Delta T(\frac{a}{h})^2$	$\left[\frac{|\Delta p|}{E}(\frac{a}{h})^4\right]^{2/3}$	$(\frac{q}{\beta E})^{1/3}\frac{a}{h}$	ψ	Flutter start or stop	Panel condition
10	0.055	1.4	358	454	99	681	17	117	0.05	0.34	24	13	140	0.54	68	39	3.94	55	Start	Flat
					58	399	10	69	.06	.41	104	58	---	---	294	43	3.30	523	Stop	Buckled
11	.055	1.4	351	450	59	406	10	69	.06	.41	31	17	130	.33	86	43	3.32	77	Start	Flat
					59	406	10	69	.04	.28	98	55	---	---	275	34	3.32	480	Stop	Buckled
19	.080	2.03	405	480	134	923	23	158	.00	.00	37	21	210	.34	50	0	3.00	79	Start	Flat
					133	915	23	158	.10	.69	86	48	---	---	115	22	2.9?	212	Stop	Buckled
20	.080	2.03	436	498	119	819	20	138	.02	.14	52	29	210	.27	69	8	2.88	98	Start	Flat
					119	819	20	138	.02	.14	100	56	---	---	133	6	2.88	218	Stop	Buckled
21	.080	2.03	405	480	100	689	17	117	.01	.07	49	27	210	.25	65	5	2.71	96	Start	Flat
					99	681	17	117	.01	.07	77	43	---	---	103	5	2.71	169	Stop	Buckled
22	.080	2.03	504	535	70	482	12	83	.05	.34	59	33	190	.17	78	13	2.41	106	Start	Flat
					70	482	12	83	.07	.48	72	40	---	---	96	17	2.41	175	Stop	Buckled
23	.080	2.03	496	531	60	413	10	69	.03	.21	63	35	190	.15	83	10	2.29	118	Start	Flat
					60	413	10	69	.03	.21	66	37	---	---	87	9	2.29	152	Stop	Buckled

(b) $q_{x,av} = 80$; $q_{y,av} = 24$; $C = 0.82$

Test	h (in.)	h (mm)	T_t (°F)	T_t (°K)	p_t (psia)	p_t (kN/m²)	q (psi)	q (kN/m²)	Δp (psi)	Δp (kN/m²)	ΔT (°F)	ΔT (°K)	f, Hz	g_a	$\alpha \Delta T(\frac{a}{h})^2$	$\left[\frac{|\Delta p|}{E}(\frac{a}{h})^4\right]^{2/3}$	$(\frac{q}{\beta E})^{1/3}\frac{a}{h}$	ψ	Flutter start or stop	Panel condition
1	0.052	1.32	453	507	154	1060	26	179	0.26	1.79	48	27	150	0.89	135	123	4.59	54	Start	Flat
6	.054	1.37	306	425	100	689	17	117	.03	.21	24	13	160	.58	69	25	4.01	78	Start	Flat
7	.054	1.37	308	426	199	1370	34	234	.23	1.58	42	23	170	1.16	120	115	5.05	41	Start	Flat
8	.054	1.37	315	430	139	956	24	165	.08	.55	27	15	170	.80	80	55	4.48	55	Start	Flat
					63	434	11	76	.01	.07	122	68	---	---	356	6	3.43	570	Stop	Buckled
9	.055	1.4	364	458	197	1355	34	234	.26	1.79	42	23	150	1.08	119	115	4.95	40	Start	Flat
					108	745	19	131	.27	1.86	150	83	---	---	422	119	4.04	800	Stop	Buckled
14	.063	1.6	406	481	155	1068	27	186	.10	.69	34	19	180	.63	86	42	4.00	82	Start	Flat
					154	1060	26	179	.03	.21	121	67	---	---	258	19	3.92	430	Stop	Buckled
24	.102	2.59	359	455	188	1294	32	220	.05	.34	98	54	260	.30	82	8	2.66	119	Start	Flat
26	.102	2.59	350	450	139	956	24	165	.09	.62	104	58	240	.22	87	11	2.39	123	Start	Flat
27	.102	2.59	403	479	99	681	17	117	.06	.41	106	59	230	.15	89	8	2.15	130	Start	Flat
28	.102	2.59	401	478	79	544	14	96	.12	.83	113	63	220	.12	95	14	1.99	133	Start	Flat
29	.102	2.59	401	478	59	406	10	69	.14	.96	116	64	210	.09	97	15	1.80	135	Start	Flat
					59	406	10	69	.03	.21	128	71	---	---	107	4	1.80	174	Stop	Buckled

TABLE II.- PANEL FLUTTER TEST DATA FOR a/b = 3.3 — Concluded

(c) $q_{x,av} = \infty$; $q_{y,av} = \infty$; C = 0.83

Test	h in.	mm	T_t °F	°K	p_t psia	kN/m²	q psi	kN/m²	Δp psi	kN/m²	ΔT °F	°K	f, Hz	g_a	$\alpha \Delta T\left(\frac{a}{h}\right)^2$	$\left[\frac{\Delta p}{E}\left(\frac{a}{h}\right)^4\right]^{2/3}$	$\left(\frac{q}{\beta E}\right)^{1/3}\frac{a}{h}$	ψ	Flutter start or stop	Panel condition
2	0.053	1.35	305	425	157	1081	27	186	0.15	1.03	32	18	170	0.98	99	88	4.75	41	Start	Flat
3	.053	1.35	316	431	94	646	16	110	.05	.34	26	14	170	.57	80	41	4.00	73	Start	Flat
4	.053	1.35	306	425	59	406	10	69	.05	.34	31	17	160	.36	92	41	3.43	90	Start	Flat
					59	406	10	69	.01	.07	118	66	---	---	358	15	3.43	586	Stop	Buckled
5	.054	1.37	302	423	70	482	12	83	.05	.34	32	18	170	.40	95	40	3.55	98	Start	Flat
					91	626	16	110	.09	.62	138	77	---	---	403	60	3.89	716	Stop	Buckled
12	.063	1.6	355	453	58	399	10	69	.00	.00	41	23	190	.24	77	0	2.87	122	Start	Flat
					60	413	10	69	.03	.21	105	58	---	---	226	10	2.89	370	Stop	Buckled
13	.063	1.6	406	481	80	551	14	96	.01	.07	36	20	180	.38	77	9	3.19	110	Start	Flat
15	.065	1.65	314	430	94	646	16	110	.04	.28	46	26	190	.38	90	23	3.27	112	Start	Flat
					94	646	16	110	.05	.34	99	55	---	---	200	25	3.26	350	Stop	Buckled
16	.065	1.65	306	425	139	956	24	165	.05	.34	34	19	190	.55	68	25	3.71	75	Start	Flat
17	.076	1.93	359	455	94	646	16	110	.01	.07	53	29	200	.27	77	3	2.80	118	Start	Flat
					57	392	10	69	.04	.28	92	51	---	---	140	13	2.37	239	Stop	Buckled
18	.076	1.93	357	454	84	578	14	96	.03	.21	64	36	200	.24	90	9	2.69	130	Start	Flat
					84	578	14	96	.01	.07	97	54	---	---	143	3	2.69	231	Stop	Buckled
25	.102	2.59	354	452	148	1020	25	172	.09	.62	103	57	240	.23	86	8	2.44	127	Start	Flat

TABLE III.- PANEL FLUTTER TEST DATA FOR a/b = 3.7, $q_{x,av} = \infty$, $q_{y,av} = \infty$, and C = 0.80

$$\left[E = 10.5 \times 10^6 \text{ psi} \quad (72.4 \text{ GN/m}^2); \quad \alpha = 12.6 \times 10^{-6} \, ^\circ F^{-1} \quad \left(22.7 \times 10^{-6} \, ^\circ K^{-1}\right)\right]$$

Test	h in.	h mm	T_t °F	T_t °K	p_t psia	p_t kN/m²	q psi	q kN/m²	Δp psi	Δp kN/m²	ΔT °F	ΔT °K	f, Hz	g_a	$\alpha \Delta T\left(\frac{a}{h}\right)^2$	$\left[\frac{|\Delta p|}{E}\left(\frac{a}{h}\right)^4\right]^{2/3}$	$\left(\frac{q}{\beta E}\right)^{1/2}\frac{a}{h}$	ψ	Flutter start or stop	Panel condition
1	0.054	1.37	300	421	159	1095	39	269	0.00	0.00	16	9	210	1.87	47	0	4.77	74	Start	Flat
					155	1068	38	262	.10	.69	138	77	---	---	380	64	4.64	680	Stop	Buckled
2	.054	1.37	305	425	119	820	29	200	.04	.28	34	19	200	1.40	99	35	4.24	112	Start	Flat
3	.054	1.37	315	430	80	551	20	138	.02	.14	41	23	200	.94	102	23	3.72	133	Start	Flat
					60	413	15	103	.03	.21	103	57	---	---	298	30	3.39	430	Stop	Buckled
4	.054	1.37	400	478	69	475	17	117	.09	.62	49	27	200	.77	143	63	3.55	145	Start	Flat
					69	475	17	117	.05	.34	123	68	---	---	358	40	3.55	616	Stop	Buckled
5	.064	1.62	400	478	159	1095	39	269	.05	.34	42	23	220	1.77	88	18	3.95	117	Start	Flat
					158	1089	39	269	.24	1.65	120	67	---	---	251	74	3.94	514	Stop	Buckled
6	.064	1.62	310	427	84	578	14	96	.00	.00	47	26	240	.99	101	0	3.24	160	Start	Flat
					84	578	14	96	.01	.07	106	59	---	---	230	9	3.24	375	Stop	Buckled
7	.064	1.62	350	450	69	475	12	83	.01	.07	63	35	205	.79	134	6	3.05	152	Start	Flat
					69	475	12	83	.01	.07	109	60	---	---	232	6	3.05	373	Stop	Buckled
8	.064	1.62	355	453	59	406	10	69	.05	.34	61	34	200	.67	135	27	2.86	179	Start	Flat
					59	406	10	69	.00	.00	79	44	---	---	170	0	2.86	269	Stop	Buckled
9	.064	1.62	350	450	64	441	11	76	.09	.62	72	40	200	.73	145	39	2.96	180	Start	Flat
					64	441	11	76	.02	.14	80	44	---	---	171	15	2.96	290	Stop	Buckled
					188	1295	32	220	.23	1.58	152	84	200	---	325	75	4.26	605	Start	Buckled

0.156(0.40)aluminum-alloy rivets

Frame

Panel skin

$a = \dfrac{26.00}{(66.04)}$

28.98
(73.60)

0.031(0.08) fiber-glass insulation

Mounting
screw

Rivet

0.01
(0.03)

1.25
(3.20)

h

0.375
(0.96)

0.49
(1.25)

1.74
(4.42)

0.25
(0.63)

Section A—A

Typical of all edges

a/b	B	b	h
3.3	10.86 (27.6)	7.88 (20.1)	0.052(0.13)
			.053(.13)
			.054(.14)
			.055(.14)
			.063(.16)
			.065(.17)
			.076(.19)
			.080(.20)
			.102(.26)
3.7	10.01 (25.4)	7.03 (17.9)	0.054(0.14)
			.064(.16)

Table of dimensions

0.24
(0.61)

0.24
(0.61)

0.50
(1.27)

0.50
(1.27)

Rivet spacing

Figure 1.- Panel construction details (typical of all panels). All dimensions are in inches (cm).

Protective doors

Filler plates

Test panel
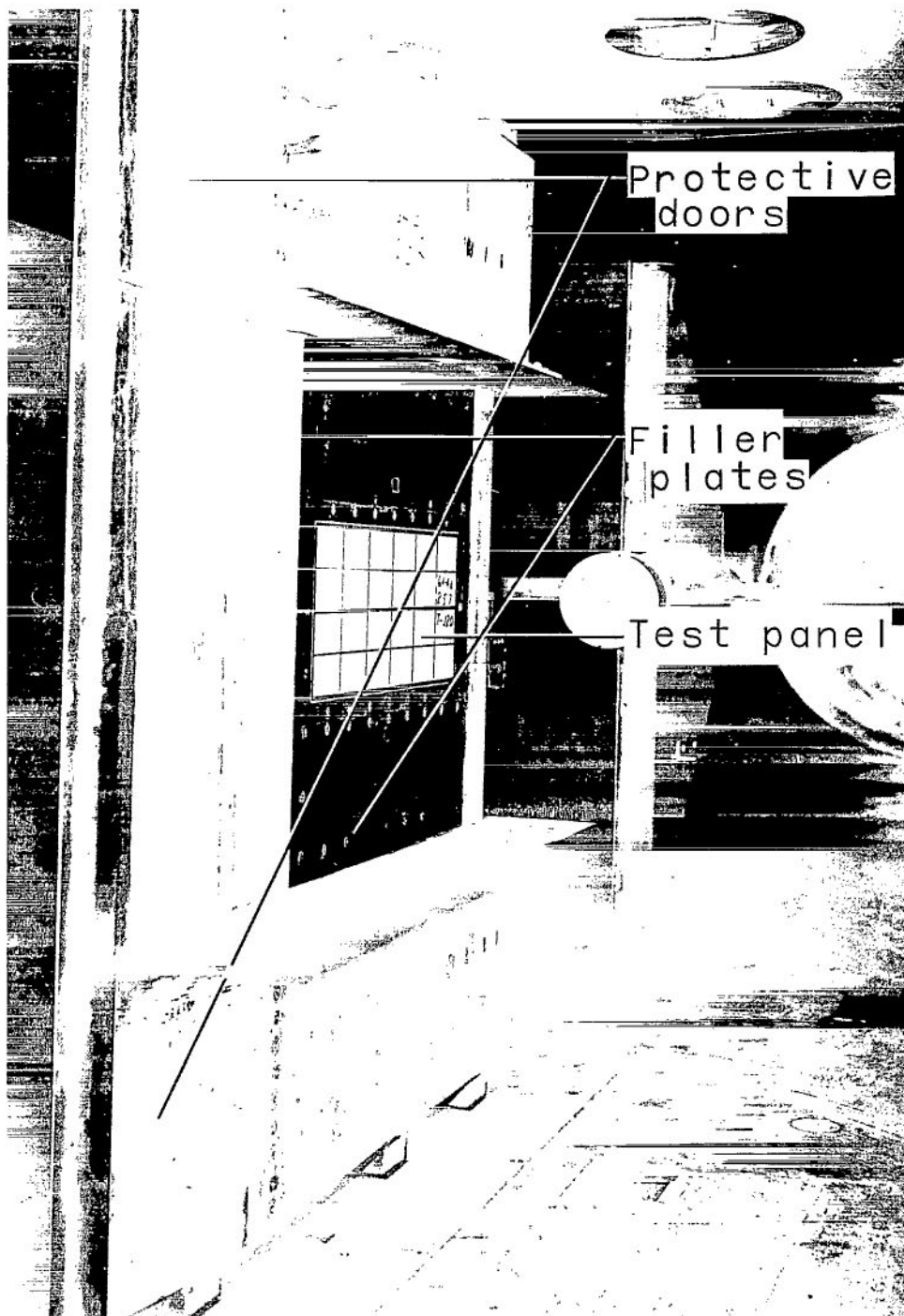
Figure 2.- Panel holder in test section as viewed from upstream.   L-64-2337.1
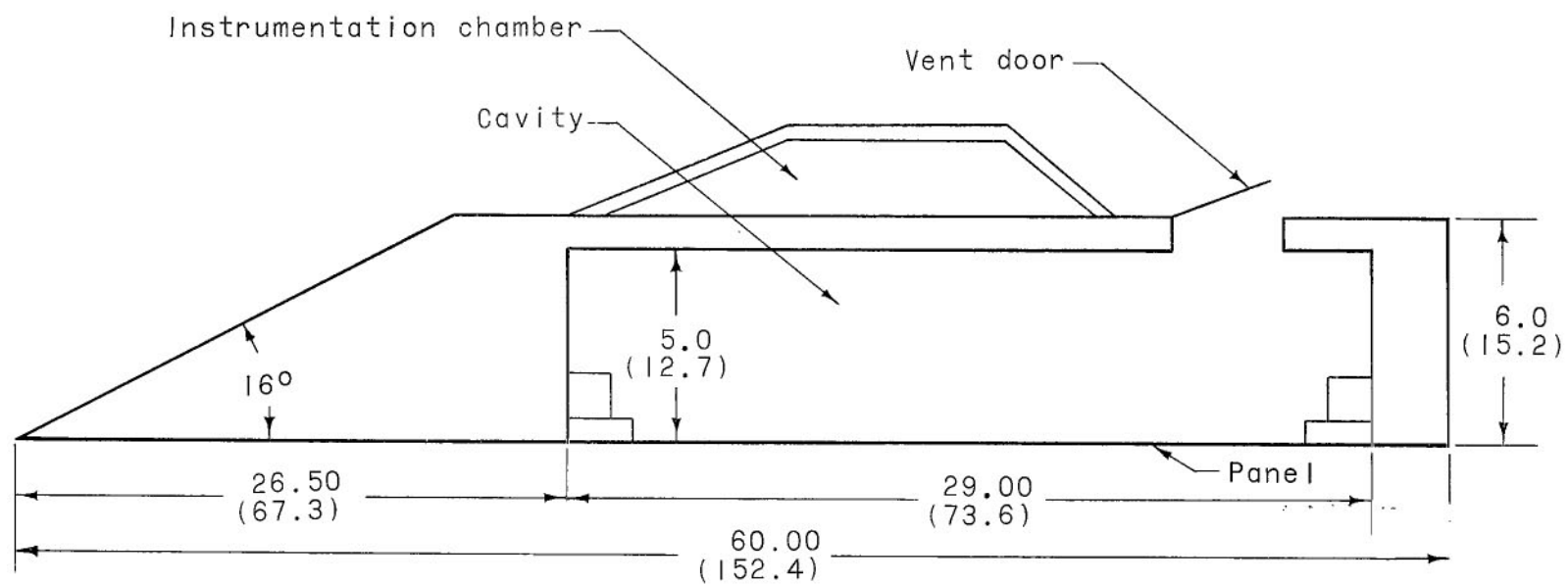
Figure 3.- Cross section of panel holder. All dimensions are in inches (cm).
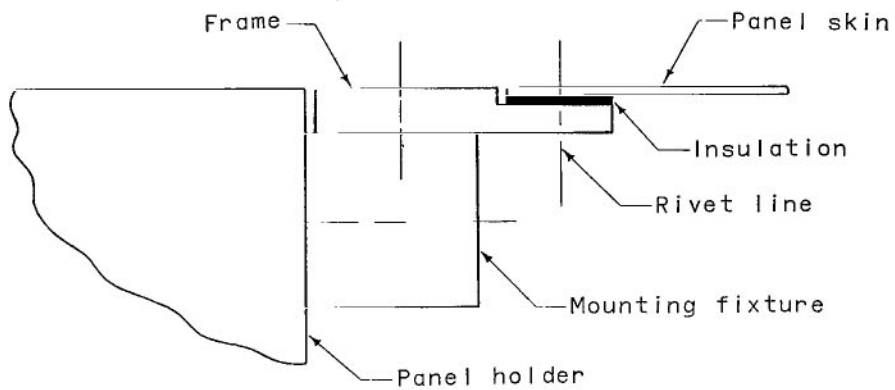
(a) Leading- and trailing-edge detail.
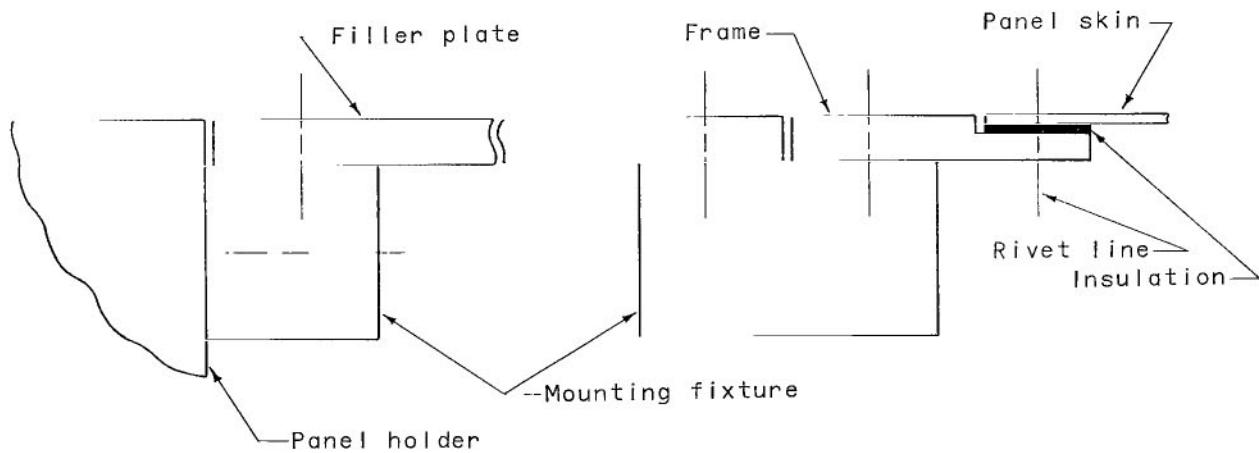
(b) Side-edge detail.

Figure 4.- Panel mounting arrangement (typical of all panels).
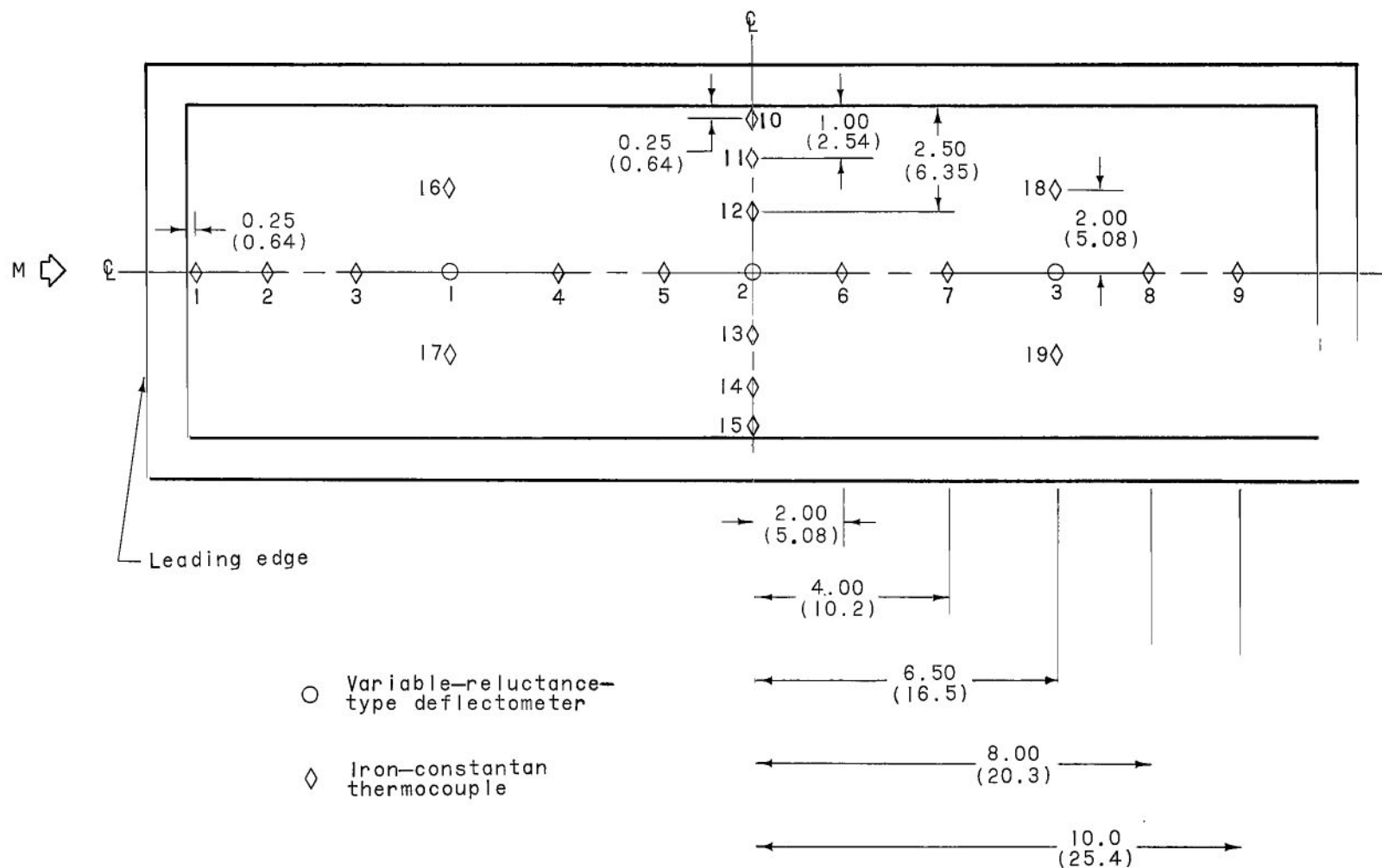
Figure 5.- Location of panel instrumentation (typical of all panels). All dimensions are in inches (cm).
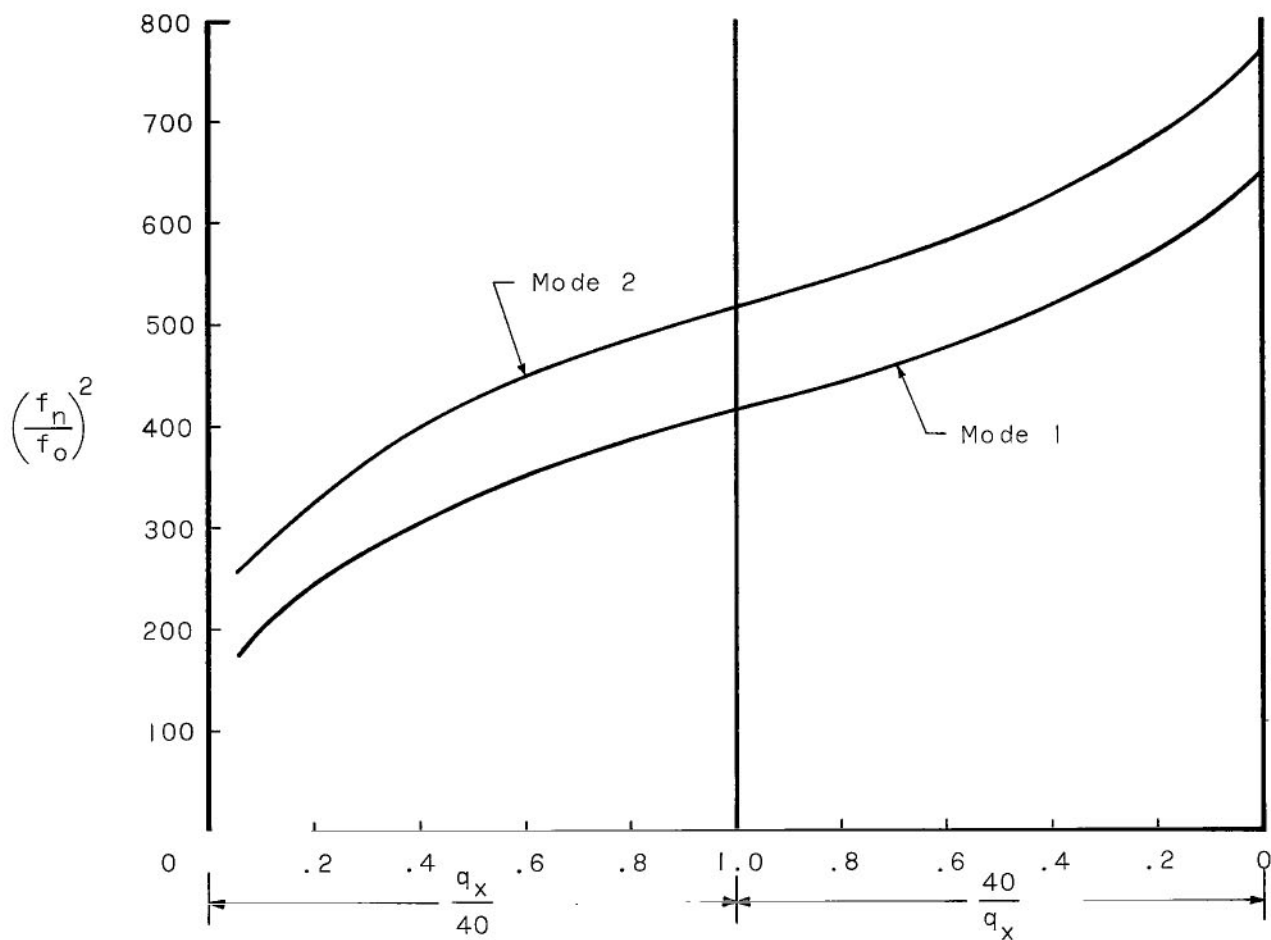
Figure 6.- Variation of frequency ratio with q_x. $a/b = 3.3$; $N_y/N_x = 1$; $\theta_x = \theta_y$.
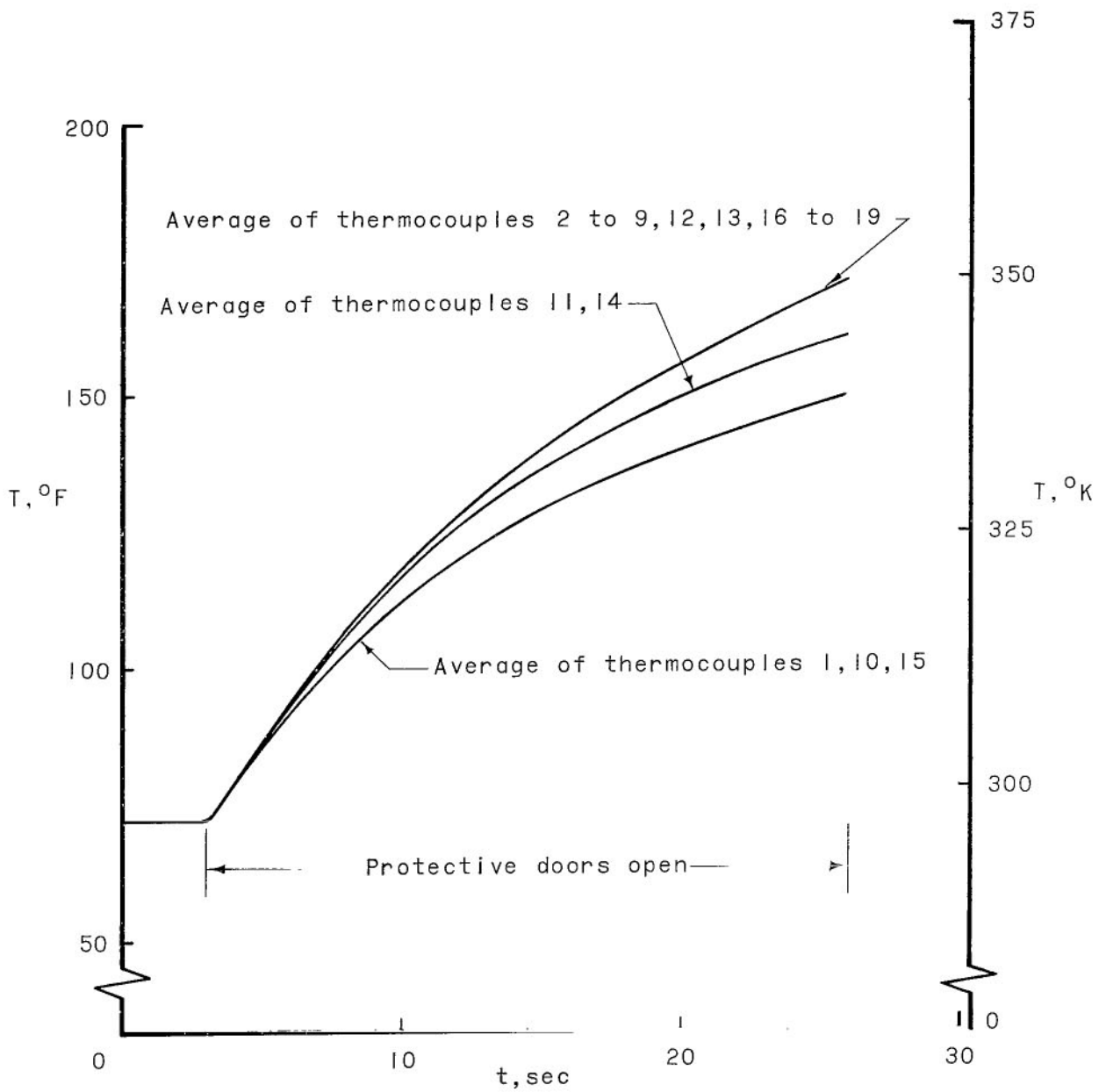
Figure 7.- Typical panel temperature history.
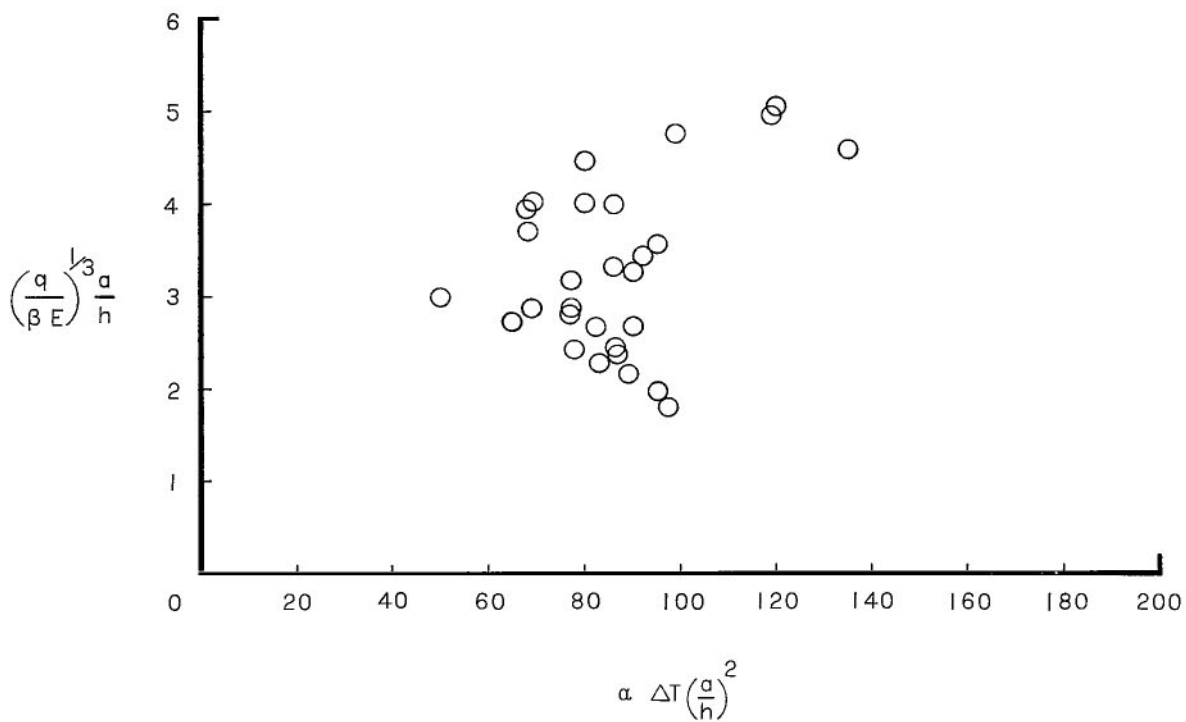
Figure 8.- Experimental flutter-start points uncorrected for Δp effects. a/b = 3.3.
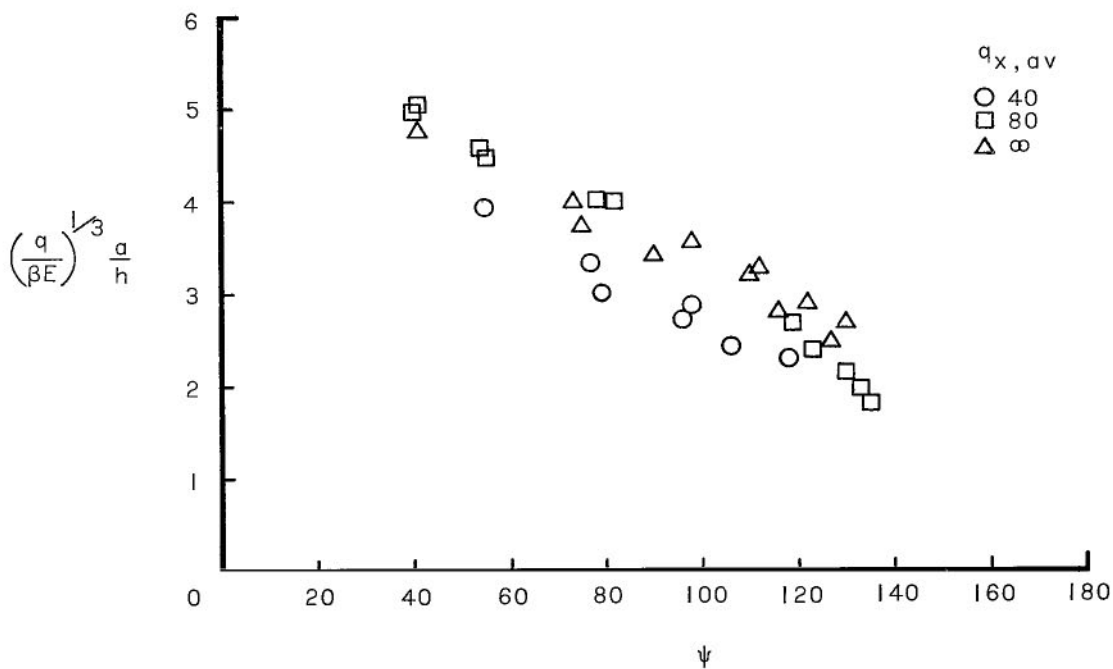
Figure 9.- Experimental flutter-start points grouped according to values of $q_{x,av}$ and corrected for Δp effects. a/b = 3.3.
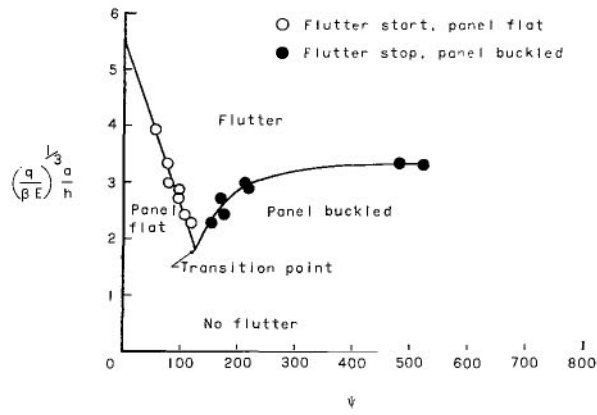
(a) $q_{x,av} = 40$.
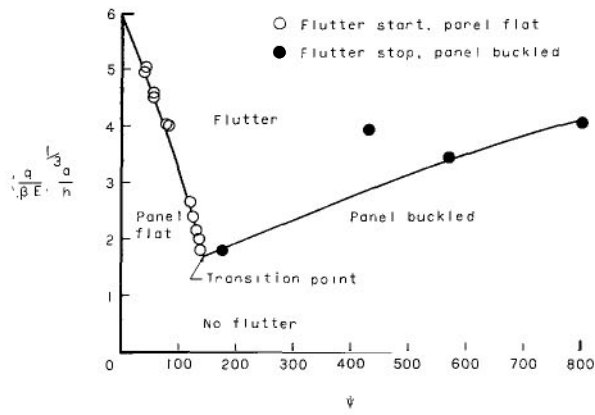
(b) $q_{x,av} = 80$.
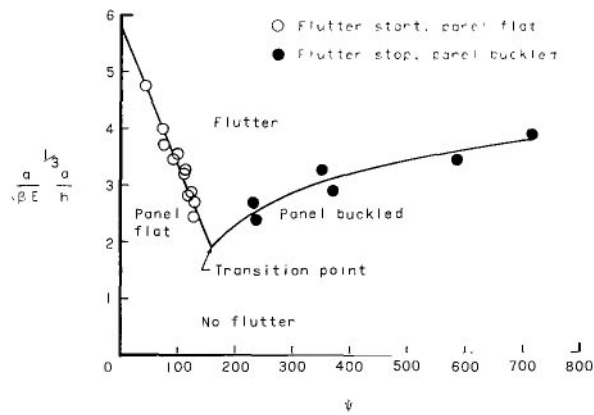
(c) $q_{x,av} = \infty$.

Figure 10.- Experimental flutter boundaries. $a/b = 3.3$; $N_y/N_x = 1$; $\theta_x = \theta_y$.
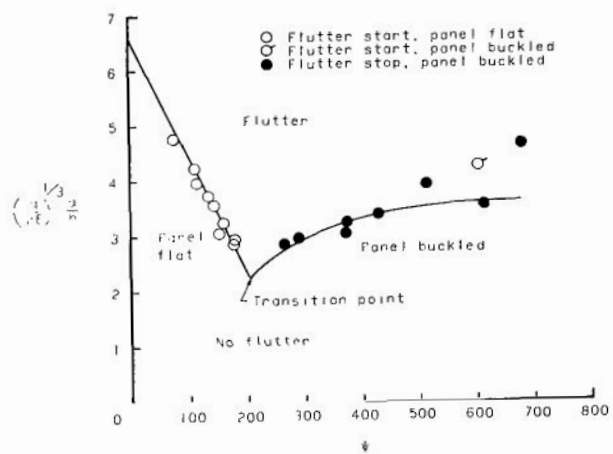
Figure 11.- Experimental flutter boundary. $a/b = 3.7$; $N_y/N_x = 1$; $\theta_x = \theta_y$; $q_{x,av} = \infty$.
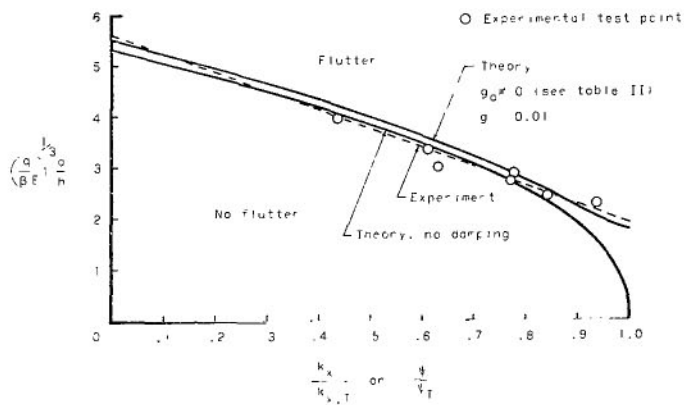
(a) $q_{x,av} = 40$.
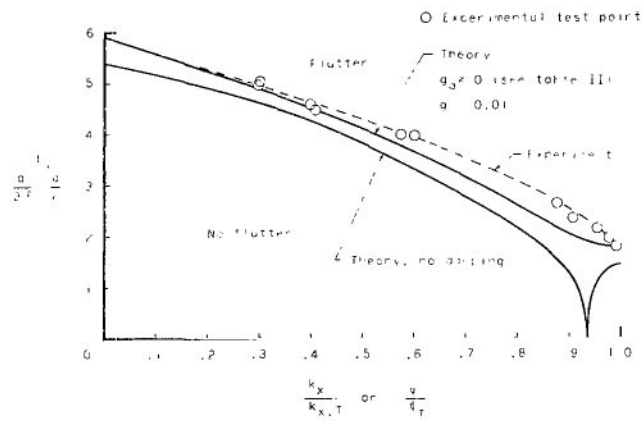
(b) $q_{x,av} = 80$.
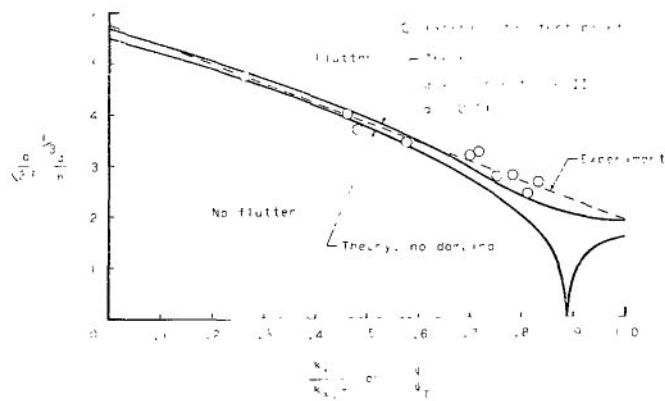
(c) $q_{x,av} = \infty$.

Figure 12.- Comparison of panel-flat portion of experimental flutter boundaries in figure 10 with theoretical flutter boundaries. $a/b = 3.3$; $N_y/N_x = 1$; $\theta_x = \theta_y$.

Figure 13.- Comparison of panel-flat portion of experimental flutter boundary in figure 11 with theoretical flutter boundaries. $a/b = 3.7$; $N_y/N_x = 1$; $\theta_x = \theta_y$; $q_{x,av} = \infty$.
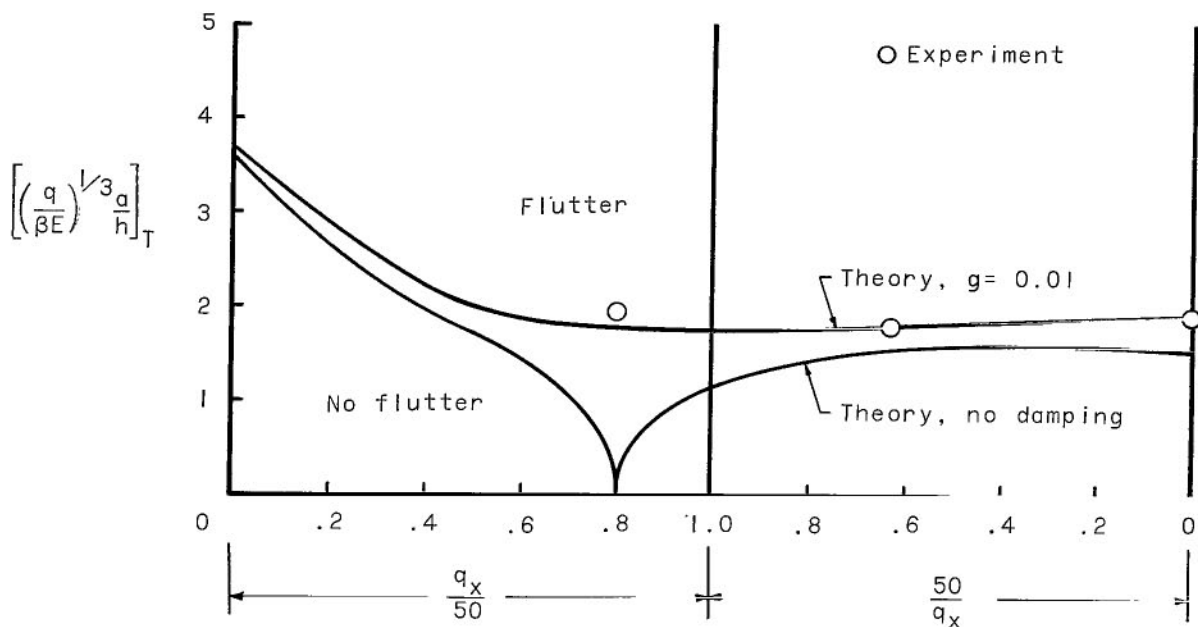
Figure 14.- Effect of edge rotational restraint on transition-point flutter. $a/b = 3.3$; $N_y/N_x = 1$; $\theta_x = \theta_y$.
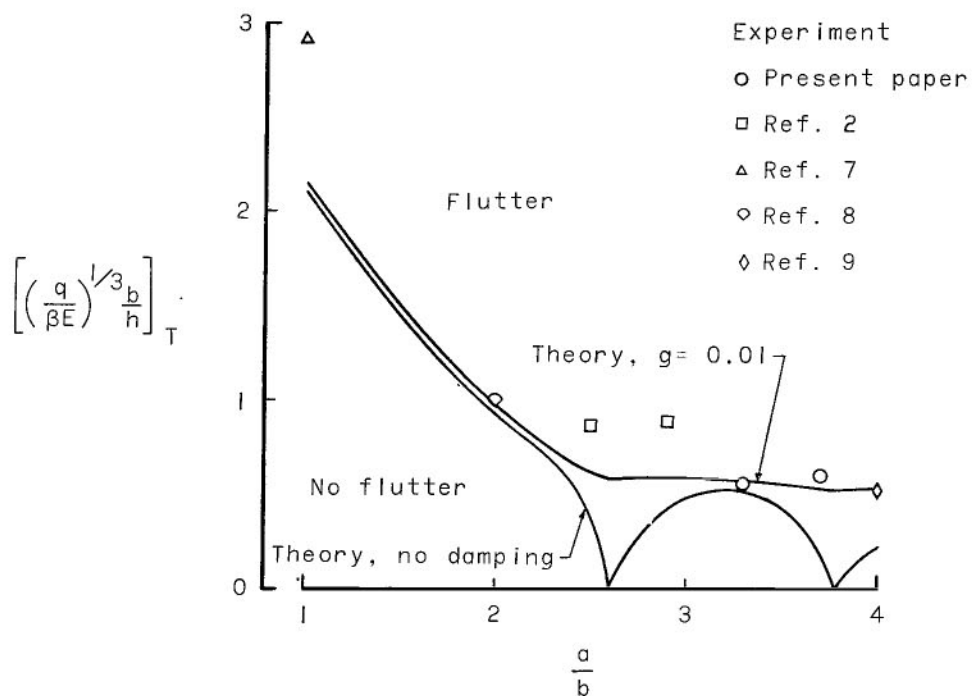

Figure 15.- Effect of length-width ratio on transition-point flutter. $N_y/N_x = 1$; all edges clamped.

"The aeronautical and space activities of the United States shall be conducted so as to contribute . . . to the expansion of human knowledge of phenomena in the atmosphere and space. The Administration shall provide for the widest practicable and appropriate dissemination of information concerning its activities and the results thereof."

— NATIONAL AERONAUTICS AND SPACE ACT OF 1958

NASA SCIENTIFIC AND TECHNICAL PUBLICATIONS

TECHNICAL REPORTS: Scientific and technical information considered important, complete, and a lasting contribution to existing knowledge.

TECHNICAL NOTES: Information less broad in scope but nevertheless of importance as a contribution to existing knowledge.

TECHNICAL MEMORANDUMS: Information receiving limited distribution because of preliminary data, security classification, or other reasons.

CONTRACTOR REPORTS: Scientific and technical information generated under a NASA contract or grant and considered an important contribution to existing knowledge.

TECHNICAL TRANSLATIONS: Information published in a foreign language considered to merit NASA distribution in English.

SPECIAL PUBLICATIONS: Information derived from or of value to NASA activities. Publications include conference proceedings, monographs, data compilations, handbooks, sourcebooks, and special bibliographies.

TECHNOLOGY UTILIZATION PUBLICATIONS: Information on technology used by NASA that may be of particular interest in commercial and other non-aerospace applications. Publications include Tech Briefs, Technology Utilization Reports and Notes, and Technology Surveys.

Details on the availability of these publications may be obtained from:

SCIENTIFIC AND TECHNICAL INFORMATION DIVISION

NATIONAL AERONAUTICS AND SPACE ADMINISTRATION
Washington, D.C. 20546